DOI: https://doi.org/10.52973/rcfcv-e32119 Revista Científica, FCV-LUZ / Vol. XXXII, rcfcv-e32119, 1 - 13

A new crotamine-like from the rattlesnake (*Crotalus durissus cumanensis*) venom causing damages: Qualitative and Quantitative Cytotoxic Studies on subcellular and neuromuscular structures

Una nueva crotamina similar de la serpiente de cascabel (*Crotalus durissus cumanensis*) causante de daños: estudios citotóxicos cualitativos y cuantitativos en estructuras sub-celulares y neuromusculares

***Estefanie García*[1], *Héctor José Finol*[1†], *Roschman González*[1] *and Alexis Rodríguez-Acosta*[2*]**

[1]*Universidad Central de Venezuela, Faculty of Sciences, Electron Microscopy Centre. Caracas, Bolivarian Republic of Venezuela.* [2]*Universidad Central de Venezuela, Anatomical Institute, Laboratory of Immunochemistry and Ultrastructure. Caracas, Bolivarian Republic of Venezuela.*
**Email: rodriguezacosta1946@yahoo.es*

ABSTRACT

A quantitative model to expose the adrenal gland sub-cellular alterations produced by crotamine-like (C-L) from rattlesnake venom during 3, 6 and 24 hours (h), and also qualitative changes on mice neuromuscular structures *in vivo* were observed and calculated by transmission electron microscopy. A pure crotamine-like (C-L) isoform was obtained using a cationic exchange chromatography column from the rattlesnake *Crotalus durissus cumanensis* venom. The C-L SDS-PAGE (15.5 %) under non-reduced conditions exhibited a molecular mass of ~3 kDa single band. The C-L *in vivo* qualitative experiments induced ultrastructural changes in mouse neuromuscular structures at 3, 6 and 24 h, such as reduction in the number of acetylcholine vesicles, disorganisation of the secondary synaptic clefts, enlargement of the sub-sarcolemma space and alteration of the mitochondria morphology, number and cristae. Regarding neurotoxic actions *in vivo*, the animals injected with C-L presented spastic paralysis of the hind limbs. The quantitative alterations studied on the capillaries, the nucleus, the mitochondria the lipid inclusions, and the smooth endoplasmic reticulum were observed from 3 to 24 h after C-L injection. As far as it is known from the literature review, there are no quantitative records of similar sub-cellular alterations caused by crotamine.

Key words: Crotamine-like peptide; *Crotalus durissus cumanensis;* mitochondria; motor- endplate; myotoxin, rattlesnake; smooth endoplasmic reticulum

RESUMEN

Se observó y calculó mediante microscopía electrónica de transmisión, un estudio cuantitativo para exponer las alteraciones subcelulares de la glándula suprarrenal producidas por crotamina-similar (C-L) del veneno de serpiente de cascabel, durante 3; 6 y 24 horas (h), y también los cambios cualitativos *in vivo* en las estructuras neuromusculares de ratones. Se obtuvo una isoforma pura similar a la crotamina (C-L) usando una columna de cromatografía de intercambio catiónico del veneno de *Crotalus durissus cumanensis*. La SDS-PAGE (15,5 %) de la C-L en condiciones no reducidas exhibió una masa molecular de ~3 kDa de banda única. Los experimentos cualitativos *in vivo* de C-L indujeron cambios ultraestructurales, bajo microscopía electrónica en constituyentes neuromusculares de ratón a las 3; 6 y 24 h, tales como reducción en el número de vesículas de acetilcolina, desorganización de las hendiduras sinápticas secundarias, agrandamiento del espacio sub-sarcolema y alteración de las mitocondrias. En cuanto a las acciones neurotóxicas *in vivo*, los animales inyectados con C-L presentaron parálisis espástica de las extremidades posteriores. Las alteraciones cuantitativas estudiadas en los capilares, el núcleo, las mitocondrias, las inclusiones lipídicas y el retículo endoplásmico liso se observaron de 3 a 24 h después de la inyección de C-L. Hasta donde se conoce por la revisión de la literatura, no existen registros cuantitativos de alteraciones sub-celulares similares provocadas por la crotamina.

Palabras clave: Péptido similar a la crotamina; *Crotalus durissus cumanensis*; mitocondrias; placa motora terminal; miotoxina, serpiente de cascabel; retículo endoplásmico liso

Received: 19/02/2021 Accepted: 04/04/2022 Published: 17/05/2022

INTRODUCTION

In many Countries that are located in the tropical and sub-tropical areas, the ophitoxemia represents a serious Collective Health problem [13], and they are unfortunately included in the neglected tropical diseases. In the Neo-tropics, rattlesnakes cause about 12 % of snake envenomation [27] with significant mortality rates. One of the most neurotoxic and myotoxic components of these venoms is crotamine, causing symptoms of muscle damage and spastic paralysis in patients bitten by these species.

The symptoms of the ophitoxemia produced by the *Crotalus* snake's venoms are the consequence of the combination of several toxins effects and enzymes that framework the involved species. It is necessary to investigate their neurotoxic, myotoxic and haemostatic effects at subcellular level. Each venom of a viper species constitutes a unique mixture of peptides and proteins chosen by natural selection to act on the vital systems of its prey. These qualitative and quantitative differences between venoms exist in families, genera, species and even intra-species [1].

The venoms of *Crotalus* snakes are responsible for pathological sub-cellular lesions, which have been described by electron microscopy techniques in several previous works [2, 8, 25, 29]. It is common that in venoms scientific research there is a relationship between the enzymatic and clinical pathological pictures; however, when adding the sub-cellular level of description that offers a tool such as Electron Microscopy (EM), the understanding and the pathological analysis is necessarily improved. Indeed, the existence of studies in EM that have allowed to describe the alterations caused by venoms in various organs have been established, nevertheless, as far as it was known from the literature review, there are no quantitative records of similar sub-cellular alterations caused by crotamine.

Also, in the present work, a quantitative study measuring the action of crotamine-like (C-L) from the common rattlesnake *Crotalus durissus cumanensis* (*Cdc*), on the capillary endothelium, capillary lumen, nucleus area, nucleus envelope, number of mitochondria, Areal number density of mitochondria, number of mitochondrial cristae, number of lipid inclusions, areal number density of lipids inclusions and cisternae of the smooth endoplasmic reticulum (REL) from adrenal gland cells have been studied. On the other hand, a qualitative revision demonstrating a dynamic evolution of damages on neuromuscular structures from 3, 6 to 24 hours (h) was carried out.

MATERIALS AND METHODS

Snakes

Four males and four females of common rattlesnake (*Crotalus durissus cumanensis*) were captured at Santa Teresa del Tuy Town, Miranda State, Venezuela. Snakes were placed and well-kept at the Serpentarium of the Tropical Medicine Institute, Caracas, Venezuela.

Venom

Venom extraction was achieved by permitting the snake to chew into a para-film stretched over a disposable plastic cup. The venom was pooled, centrifuged (Allegra® X-30 Centrifuges, Beckman Coulter, USA) (500 × g for 10 minutes (min), and filtered by means of 0.45 micrometres (µm) filter, under positive pressure. The pooled venom was lyophilised and stored (Frigidaire FGVU21F8QF Vertical Freezer, USA) at –30°C until use.

Mice

Ultrastructural studies were carried out using 18 adult female NIH strain mice (*Mus musculus*) (18-22 grams – g-) purchased from the vivarium of the National Institute of Hygiene "Rafael Rangel", Caracas, Venezuela. Animals were provided with water and food *ad libitum*, until used.

Crotamine-like (C-L) purification

Purification of C-L from the rattlesnake venom was carried out by one chromatographic step [29]. Crude venom (*Cdc*) (30 milligrams-mg by protein estimation) [33] was diluted to 1.0 millilitres (mL) of 50 milli Molar (mM) Tris–HCl buffer, pH 8.2, and then applied on a Mono S HR 10/10 column (GE Healthcare Biosciences Ltd, USA) equilibrated with an equivalent buffer. Supporting proteins were eluted with a 0–1 M NaCl linear gradient in equivalent buffer over 60 min at a flow rate of 1.5 mL·min-1. Proteins were checked at 280 nanometres (nm). The chromatogram showed 8 fractions, which were identified agreeing to their elution. Well-defined spastic hind-limb paralysis action on mice was ostensible in fraction 5 (C-L), which was dialysed against water at 4°C, lyophilised and stored at –30°C and selected for the experimental assays.

Polyacrylamide gel electrophoresis (SDS-PAGE)

To support the purity of the chromatographic peaks, an electrophoresis of the *Cdc* crude venom (20 micrograms (µg) and the C-L (60 µg) was performed on analytical discontinuous gels with 12.5 % separation and non-reducing conditions. The gels were stained with a Coomassie blue staining solution. Densitometry of the gels was performed using a GS-690 Densitometer (BIO-RAD, USA) and the analysis of the profile of the proteins and their molecular masses were determined using the Multi-Analyst version 1.1 program (BIO-RAD, USA).

Protein concentration

Protein concentration of C-L was spectrophotometric measured, accepting that 1 unit of absorbance/centimeters (cm) of wavelength at 280 nm corresponds to 1 mg protein·mL^{-1} [33].

Procedure for qualitative study of specimens by electron microscopy (TEM)

For the qualitative study, 18 adult female NIH strain mice (18-22 g) were divided in two groups: the normal control (n=9) in which mice were injected intravenously (i.v.) (in the central tail vein) with 0.1 mL of saline solution and the experimental group (n=9) also injected via i.v. with 20 µg·mL^{-1} of C-L in 100 µL of phosphate buffer saline (PBS). After 3, 6 and 24 h, three mice from each group were prepared for motor end-plate of striated muscle (muscles of the hind-limb) biopsies. The fragments were obtained from control and experimental mice immediately after to be sacrificed by cervical dislocation. Samples were straightaway *in situ* fixed with 3 % glutaraldehyde and 1 % OsO_4 (both fixatives diluted in 320 mM phosphate buffer saline, pH 7.4), dehydrated in ethanol and embedded in LX-112 resin (Ladd Research Inc.). Ultrathin sections were stained with uranyl acetate and lead citrate and observed with a FEI, TecnaiSpirit 12G2 model, (University of Minnesota, College of Engineering, USA) transmission electron microscope with an accelerating voltage of 100 kilovolts (kV).

Procedure for quantitative study specimens by principal component analysis (PCA)

Principal component analysis (PCA) consisted of expressing a collection of variables in a set of linear combinations of factors not correlated with each other [12, 38]. This method allowed the original data (individuals and variables) to be represented in a space with a dimension less than the original space [12, 38].

Digitisation of the image

In order to carry out a descriptive quantitative study of the biological sample (The capillaries, the nucleus, the mitochondria the lipid inclusions, and the smooth endoplasmic reticulum) from a micrograph, the magnification handled for their registration was pondered, as well as the magnification factor, with which the revealed physical image was acquired. By means of the "mouse" (Mouse laser Bluetooth ThinkPad, China) it was delineated points, the length, the angle, the area, among others, in the image acquired directly from the TEM, so that the object in the image could be determined in real time. Thus the images pick up directly from the electron microscope were used to the quantitative study. The structures appraised with the TEM were processed with the computer to analyse and classify the data using statistical programs (see below). The structures were included and preserved sizes according to the original magnification, with which it was reached. The images obtained by the FEI Quanta 250 FEG electron microscopy (USA) were gathered digitally in a computer for further study.

Considered usage of the results

Image J

From the micrographs procured in the thin and thick sections, morphometric magnitudes were done through the Image J software (National Institutes of Health, Bethesda, MD, USA).

The images obtained from the FEI Quanta 250 FEG equipment were analysed by using the IMAGE J program, which from the micro-mark supplied in each image allows carried out morphometric measurements. From each sampling point, 30 digital images that generated 40 measurements were obtained at each time of each treatment (3, 6 and 24 h).

Statistical analysis

The statistics were carried out by ANOVA statistical technique, which is used to associate a probability, with the notion, that the mean of a group of scores is different, from the mean of another group of scores. Through the comparison, it was tested a hypothesis of difference between more than two groups [6]. To apply the ANOVA it was used *a priori* Levene's tests (Levene's Test for Homogeneity of Variances). To corroborate the homogeneity of variance and for normality, the Kolmogorov-Smirnov test with Lilliefors correction was used and the histograms were also verified.

To consider the dependent morphometric and other variables analysed: Capillary endothelium, Capillary lumen, Nucleus area, Nucleus envelope, Number of mitochondria·μm^{-2}, Areal number density of mitochondria, Mitochondria cristae, Number of lipid inclusions·μm^{-2}, Areal number density of lipids inclusions, Diameter smooth endoplasmic reticulum (SER), two-way analysis of variance (2-way ANOVA) was used by Sokal and Rohlf [18, 31]. Two independent variables (2 factors) were taken in each analysis: the first "the group" (Control and C-L and the second "the time" (6,12 and 24 h). For the application of each ANOVA, the prior assumptions or tests of normality and homogeneity were corroborated, using a confidence of 95 % (significance 0.05). Obtaining a total of 6 treatments (2 groups with 3 time each). In the cases in which the ANOVA indicated statistically significant differences, the posterior test of Minimal significant differences (MSD) was used. The results of these tests indicated in tables 1 to 10 show letters that specify the 6 treatment groups that have statistically significant differences. These tables also show the descriptive statistics for each variable (arithmetic mean and standard error) (STATISTICA V.8.0 Program).

Principal component analysis (PCA)

The PCA was defined by the expressing of a set of variables, in an arrangement of linear combinations of factors, which were not correlated among them. This process allowed to symbolise the original data (individuals and variables), in a space of fewer dimensions than the original space. The variables, for the quantitative description of the thickening of the capillary endothelium, area of capillary lumen, swelling of the perinuclear space, nucleus envelope, number of mitochondria, Areal number density of mitochondria, number of mitochondrial cristae, number of lipid inclusions, areal number density of lipids inclusions and cisternae diameter of the smooth endoplasmic reticulum (REL) were considered (MVSP V3.0 Program).

RESULTS AND DISCUSSION

Knowing that the effects of snake venom appear in a short time in the patients and that a high rate of damage is exhibited [27], in the current work, it was planned to show the damages produced by the C-L, not only in a specific time, but then by including a chronological variable, allowing us forming a kinetics to establish an approximate time, when the cellular alterations obtained by ME occur, and comparing the variability of the alterations among the treatments with the toxin, in relation to the time. To achieve the aforementioned, three intervals were taken into account, at 3, 6 and 24 h post C-L injection. In this way, ultrastructural alterations were observed throughout the experiment, being represented in different types of sub-cellular damage. These changes were necessarily due to the action of C-L during the kinetic study, and were related to the type of ultrastructure observed and certainly associated to the symptoms and the pathology generated by the toxin [1].

Having the opportunity and possibility of describing an innovative study about the ultrastructural alterations that C-L generates on sub-cellular structures and being able to quantitatively measure them, the opportunity of observing qualitative collateral studies, related to the action of C-L on the motor endplate could not be missed.

In recent years, several neuro and myotoxins have been isolated from snake venoms, and the mechanism of action of their components has been investigated [2, 3, 8, 29], since crotamine is one of the important components of Crotalidae venom that combines cytotoxic and neurotoxic properties [5], it was carried out this study of the alterations in the neuro-motor plates produced by the action of purified C-L as described in results sections.

First of all, it was started with the C-L purification and isolation from *Cdc* venom, which was separated by Mono S HR 10/10 cationic exchange column, which produced 8 well-defined fractions (FIG. 1). The spastic inferior limbs paralysis action (conventional sign of

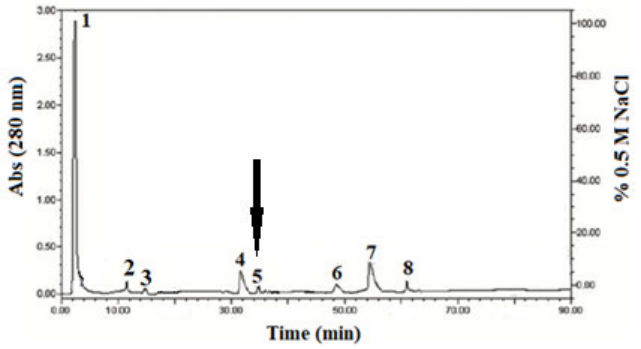

FIGURE 1. Purification and Isolation of C-L. Crotamine-like from *Crotalus durissus cumanensis* venom was isolated by Mono S HR 10/10 cationic exchange column, which produced 8 peaks The spastic inferior limbs paralysis activity (conventional sign of crotamine presence) was noticed in fraction 5 (arrow), named C-L

crotamine presence) was noticed in fraction 5, named crotamine-like (C-L). SDS-polyacrylamide gel electrophoresis (SDS-PAGE)[5] of C-L fraction (10–20 %) under non-reduced conditions showed a single band of ~3 kilodaltons (kDa) molecular mass (FIG. 2).

The action of crotamine had been studied in skeletal muscle from a pathological point of view, showing that the toxin, once inoculated intramuscularly, induced muscle contraction both *in vivo* (spastic inferior limbs paralysis) and *in vitro* [5] experiments. Crotamine, isolated from *Crotalus* snake venom act on skeletal muscle cells, combining cytotoxic and neurotoxic properties[10, 20].

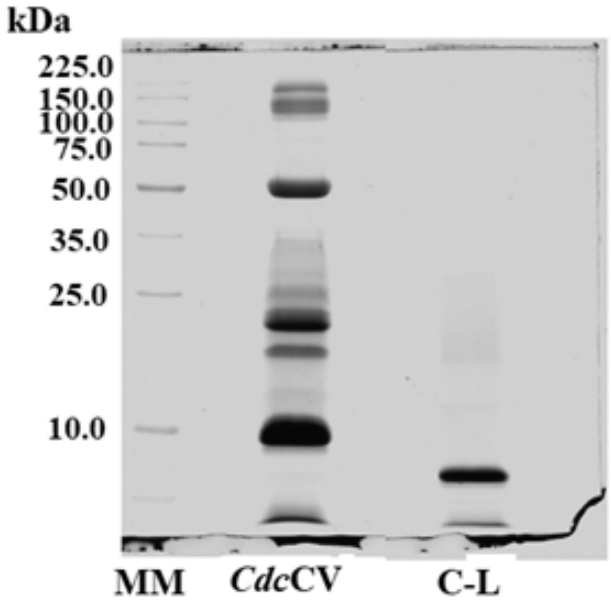

FIGURE 2. SDS-PAGE (12.5 %) of Cromatine-like under non-reduced condictions. MM: molecular masses markers; *Cdc*CV: *Crotalus durissus cumanensis* crude venom; C-L: crotamine-like

The ability of crotamine to penetrate the cell membrane varies among the different isoforms that have been described [14, 26, 35]. In these works, it was shown that the toxinological action of crotamine was carried out through nerve tissue voltage gated sodium and potassium channels [23, 24], in addition to the activation of sodium influx at muscle cells [4]; its action on skeletal muscle has represented the first snake venom peptide classified as a cell penetrating peptide and antimicrobial peptide (CPP and AMP), also demonstrating that crotamine induces skeletal muscle contraction both *in vitro*/*in vivo*, and damages in the motor endplate [24].

In the normal image of the muscle motor endplate were observed the presence of acetylcholine vesicles in an axonal terminal, mitochondria with normal ultrastructure and a secondary synaptic cleft as corresponding to a normal motor endplate structure (FIG. 3.1).

After 3 h post-C-L injection, the micrograph showed a terminal axon with few acetylcholine vesicles, secondary synaptic clefts. Mitochondria without cristae were also observed (FIG. 3.2).

After 6 h post-C-L injection, a terminal axon with scarce acetylcholine vesicles, disordered secondary synaptic cleft, free polysomes and an enlarged sub-sarcolemma region were noticed (FIG. 3.3).

After 24 h post-CL injection, the micrograph showed: (FIG. 3-4a) oblique cuts images of muscle fibres, with an enlarged sub – sarcolemma space and a terminal axon with absence of acetylcholine vesicles; secondary synaptic clefts and morphological altered mitochondria. (FIG. 3-4b) A terminal axon with cellular debris and absence of synaptic vesicles were seen. Electrondense mitochondria were also observed (FIGS. 3-4A and 4B). In the FIG. 3, it has also been included an endplate image scheme. The sequential alterations description produced by C-L at the level of the motor endplate was possible to appreciate the significant reduction in the number of acetylcholine vesicles, which expresses the severe damage to cellular function. The decrease in these acetylcholine vesicles, being involved in the contraction and relaxation processes of the muscle, could be a possible explanation for the muscular paralysis that the mouse presents a few min after inoculation with C-L. This neurotoxic action showed that the injected animals were sensitive to C-L, since they presented spastic paralysis of the hind limbs, five min after intravenous injection [22]. The mice also exhibited muscle spasms, likely caused by considerable neurotransmitter release, changes in ion channels, and inhibition of vesicular recycling [23]. These authors also proposed that crotamine acts primarily on mammalian skeletal muscle and secondarily on other excitable organs, nerve and heart, which are regularly unaffected. This paralysis presented in the mice was not permanent and disappears within a few min later. Rodent studies have shown that the motor nerve terminals [7] and muscles are particularly susceptible to activities caused by myotoxins [21].

Others subcellular components detected in the current work, such as the endoplasmic reticulum (sarcoplasmic reticulum in muscle) were severely damaged. This organelle represents the largest intracellular accumulation of calcium in skeletal muscle, and plays a fundamental role in the regulation of the phenomenon of contraction and excitation, inducing intracellular calcium concentrations during muscle contraction and relaxation [9].

On the other hand, it is possible that the depletion or decrease of the synaptic vesicles from the nervous terminal is not merely a reflection of the improved exocytosis; the increased fluidity of the nerve end membrane aided by crotamine will also inhibit or retard

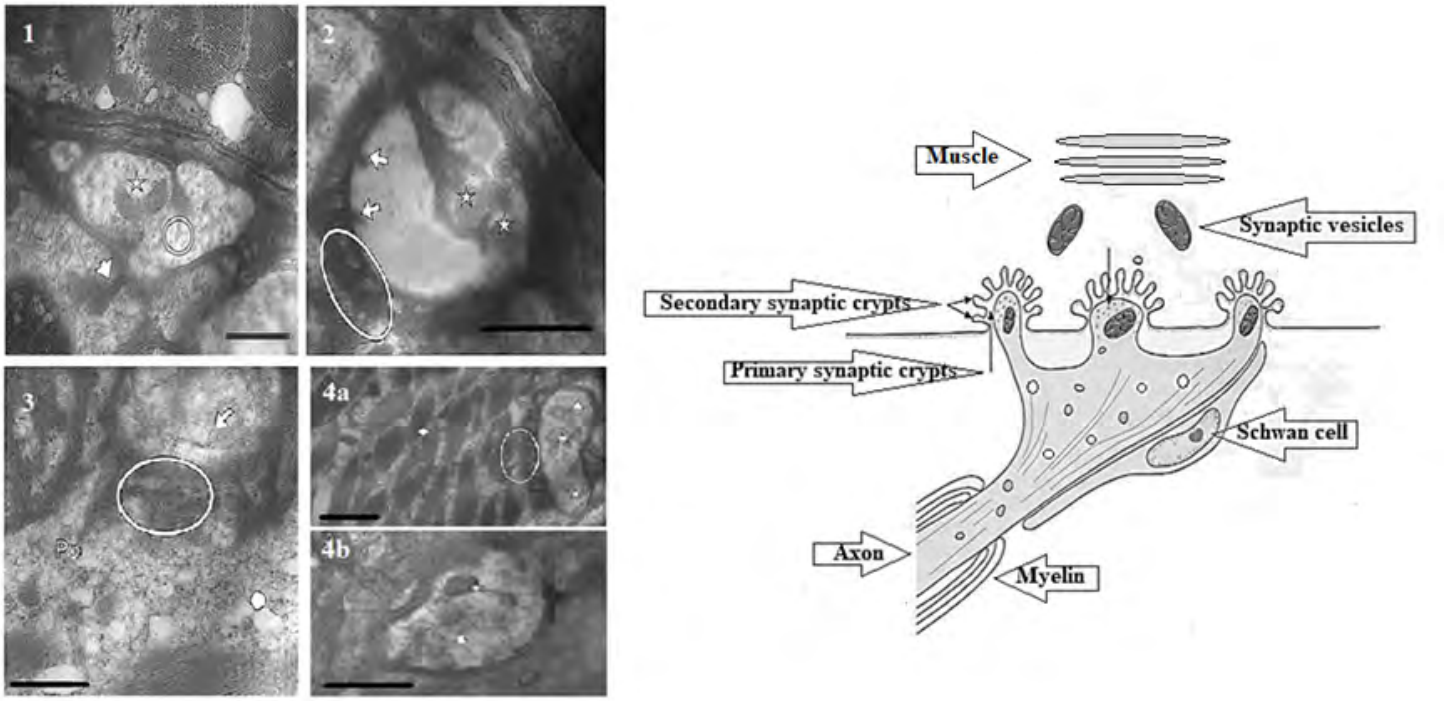

FIGURE 3. (1) Motor Endplate Normal Control and Endplate Scheme. The presence of acetylcholine vesicles can be observed (circle), it is a normal ultrastructure of axonal terminal. Mitochondria with normal cristae was seen (star); secondary synaptic cleft (arrowhead) accordingly to a motor endplate. Micromark = 1 µm. (2) Motor Endplate after 3 hours post C-L injection. The micrograph shows a terminal axon with few acetylcholine vesicles (arrow), secondary synaptic clefts (oval) and mitochondria without cristae (star) were observed Micromark = 1 µm. (3) Motor Endplate after 6 h post-C-L Injection. A terminal axon with scarce acetylcholine vesicles (arrow), disordered secondary synaptic cleft (oval); free polysomes (Po) and an enlarged sub-sarcolemma region (circle) were noticed. Micromark = 1 µm. (4) Motor Endplate after 24 h post-CL injection. The micrograph shows: (4a) oblique cuts images of muscle fibres, with an enlarged sub – sarcolemma space (circle) and a terminal axon with absence of acetylcholine vesicles (triangle); secondary synaptic clefts (oval) and altered mitochondria (star) were visualised. (4b) A terminal axon with cellular debris (triangle) and absence of synaptic vesicles was seen. Electrondense mitochondria (star) were observed Micromark = 1 µm

the recycling of synaptic vesicles. Synaptic transmission begins when an action potential or an electrochemical impulse reaches the synaptic button of the presynaptic neuron and depolarises it. In response, potential-dependent calcium channels open, allowing extracellular Ca^{2++} ions to enter and diffuse into the synaptic button. The influence of Ca^{2++} causes that many of the presynaptic vesicles, which store acetylcholine, fuse with the presynaptic membrane and thus hundreds of molecules of this substance are released by exocytosis in the cleft or synaptic space [11]. This process stops quickly because calcium ions are rapidly removed from the cytoplasm of the synaptic cleft by active transport mechanisms, and are transferred to the mitochondria, vesicles, or endoplasmic reticulum [28]; taken together, these results broaden the understanding of the procedure of action of C-L in tissues; in addition, they release new points of view for their biomedical application. Toxins that induce lysosomal cell death, a self-regulating caspase pathway, could be mostly effective in the treatment of tumour diseases.

Regarding the results of the quantitative study to calculate the C-L effect on different subcellular structures, the C-L effect on the 10 variables were described: Areal number density of mitochondria; Number of the cristae; Number of the mitochondria; Area of the nucleus; Number of Lipid Inclusions; Areal number density of lipids inclusions; Diameter of cisternae of the smooth endoplasmic reticulum; Thickening of the capillary endothelium; Capillary lumen and Nuclear envelope, which with an analysis of variances (ANOVA) of two factors (95 % confidence) were investigated. It was found that there were significant differences for changes in treatments (factor 1) P=0.00 and significant difference for the times (factor 2) P=0.00, with an interaction of P=0.00. The graph shows the tendencies of the means and standard deviations of the treatments over time. The results in the tables are shown with the means, standard deviations of each treatment, obtained in the study of the same variables, and letters that indicate the statistically significant differences derived from *a posteriori* test of minimum significant difference (MSD) (FIG. 4 to 14 and TABLES 1 to 10).

This analysis permitted, to make clear the sub-cellular alterations developed during a follow out of C-L toxic action from 3 to 24 h. The alterations were quantified by a morphometric study documenting that the C-L action, at three different intervals had statistical meaning.

Modifications of the endothelium showed an increase at 6 and 24 h compared with the normal control. Alterations of the endothelium are constantly complicated with the occurrence of haemorrhage after snake venom accidents [27]. In a different variable, the capillary lumen at six h after C-L injection showed a trivial increase, which was not statistically significant matched with the control. Although at 24 h, a kinetic of temporary increase related with a possible dilatation of

the capillary lumen respect to the control was detected. The changes of the endothelium could explain the augment of the capillary lumen at 24 h after C-L injection.

On the subject of nucleus area, at 3 and 6 h after C-L injection was not remarkably affected since a not statistically significant decrease was seen, but at 24 h the nucleus area decreased nearly 50 %. In the nucleus are the chromosomes and the genetic material. Therefore, the cell regulation of the production of enzymatic proteins using messenger RNA (mRNA), which transport the ribosomal RNA information to the cytoplasm. Crotamine-like may induce nuclear apoptosis over several ways, for instance collaboration with lysosomes to activate intracellular cell Ca^{2+} for only a short time; variation of mitochondrial membrane potential and activation of enzymes, specifically caspases, which modify the typical perform of sub-cellular assemblies and directing to cell death [16, 30]. In the observation of the number of mitochondria, a slight variation, which was not statistically significant was detected at 3 and 6 h; but, at 24 h, a strong decrease was seen. The mitochondria foremost function is to deliver the required energy to accomplish cellular respiration [37].

Concerning the areal number density of mitochondria alterations at 6 and 24 h after C-L injection an intense increase in the area was noticed, which was statistically significant compared with the control. Increases in metabolic activity during the first post injection should be accompanied by increases in the number of mitochondria, since mitochondria play an important role in the synthesis of cortical steroids, including cortisol, a hormone that increases in stress. It is considered the mitochondria as a valuable organelle that has severe ultrastructural changes that appears after the C-L injection.

TABLE I
Capillary Endothelium. Descriptive statistics of each treatment

	Time (h)	n	Mean ± SE
Crotamine-like (C-L)	3	40	0.327 ± 0.012 [c]
	6	40	0.653 ± 0.020 [b]
	24	40	0.733 ± 0.019 [a]
Sub-total (C-L)		120	0.571 ± 0.207
Normal control (N-C)	3	40	0.305 ± 0.013 [c]
	6	40	0.308 ± 0.014 [c]
	24	40	0.288 ± 0.013 [c]
Sub-total (N-C)		120	0.300 ± 0.008
Total measurements		240	

h: hours; n: number; SE: Standard error; [abc]Means with different superscripts differ according to the test of minimal significant difference (MSD) (P<0.05)

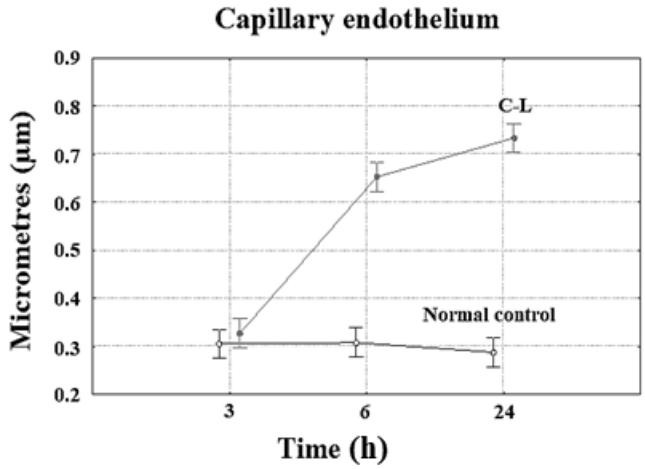

FIGURE 4. In the C-L effect on the thickening of the capillary endothelium was found significant differences in treatments (factor 1) P=0.00 and significant difference for the times (factor 2) P=0.00, with an interaction of P=0.00

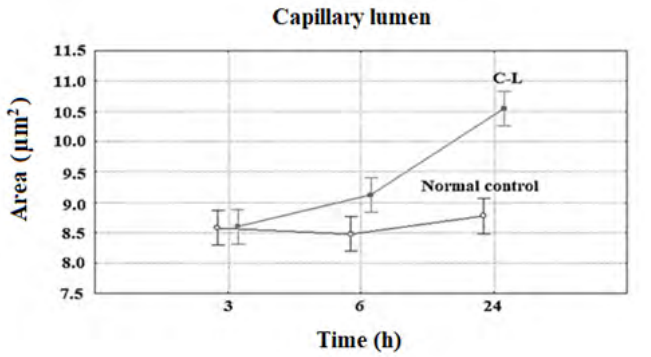

FIGURE 5. In the C-L effect on the capillary lumen was found significant differences in treatments (factor 1) P=0.00 and significant difference for the times (factor 2) P=0.00, with an interaction of P=0.00

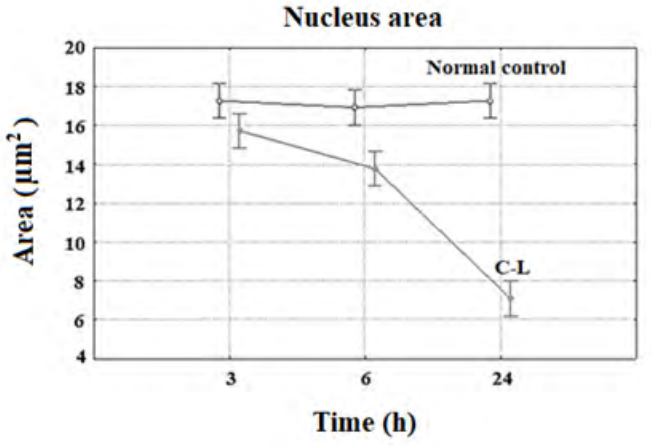

FIGURE 6. In the C-L effect on the nucleus area was found significant differences in treatments (factor 1) P=0.00 and significant difference for the times (factor 2) P=0.00, with an interaction of P=0.00

TABLE II
Capillary Lumen. Descriptive statistics of each treatment

	Time (h)	n	Mean ± SE
Crotamine-like (C-L)	3	40	8.600 ± 0.167 [c]
	6	40	9.125 ± 0.193 [b]
	24	40	10.550 ± 0.179 [a]
Sub-total (C-L)		120	9.425 ± 1.400
Normal control (N-C)	3	40	8.575 ± 0.079 [c]
	6	40	8.475 ± 0.080 [c]
	24	40	8.775 ± 0.131 [c]
Sub-total (N-C)		120	8.608 ± 0.058
Total measurements		240	

h: hours; n: number; SE: Standard error; [abc]Means with different superscripts differ according to the test of minimal significant difference (MSD) (P<0.05)

TABLE III
Nucleus Area. Descriptive statistics of each treatment

	Time (h)	n	Mean ± SE
Crotamine-like (C-L)	3	40	15.725 ± 0.268 [b]
	6	40	13.775 ± 0.698 [c]
	24	40	7.100 ± 0.479 [a]
Sub-total (C-L)		120	12.200 ± 4.909
Normal control (N-C)	3	40	17.275 ± 0.397 [a]
	6	40	16.925 ± 0.361 [a]
	24	40	17.275 ± 0.424 [a]
Sub-total (N-C)		120	17.158 ± 0.226
Total measurements		240	

h: hours; n: number; SE: Standard error; [abc]Means with different superscripts differ according to the test of minimal significant difference (MSD) (P<0.05)

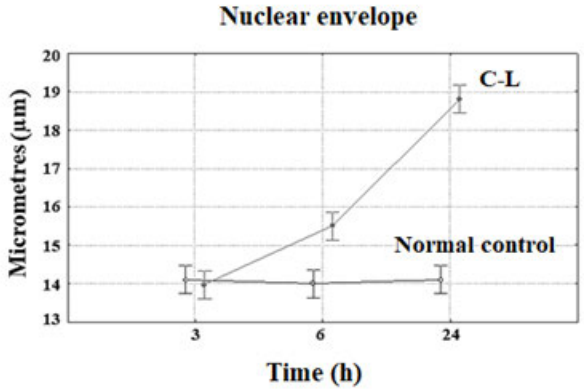

FIGURE 7. In the C-L effect on the thickening of the nuclear envelope was found significant differences in treatments (factor 1) P=0.00 and significant difference for the times (factor 2) P=0.00, with an interaction of P=0.00

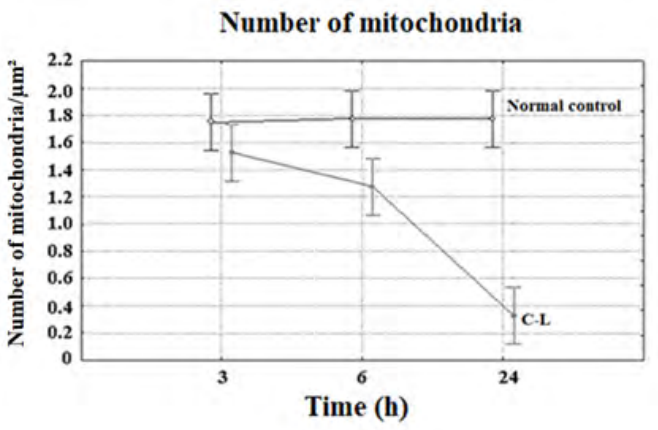

FIGURE 8. In the C-L effect on the number of mitochondria per square micrometre was found significant differences in treatments (factor 1) P=0.00 and significant difference for the times (factor 2) P=0.00, with an interaction of P=0.00

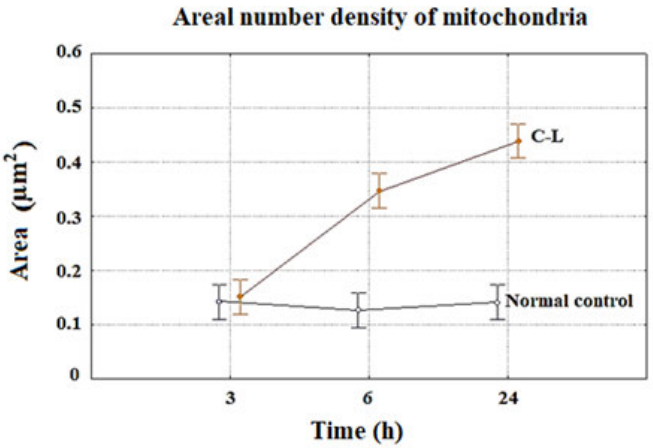

FIGURE 9. In the C-L effect on the area (µm²) number density of mitochondria was found significant differences in treatments (factor 1) P=0.00 and significant difference for the times (factor 2) P=0.00, with an interaction of P=0.00

TABLE IV
Nucleus Envelope. Descriptive statistics of each treatment

	Time (h)	n	Mean ± SE
Crotamine-like (C-L)	3	40	13.975 ± 0.288 [c]
	6	40	15.500 ± 0.139 [b]
	24	40	18.800 ± 0.224 [a]
Sub-total (C-L)		120	16.092 ± 2.467
Normal control (N-C)	3	40	14.100 ± 0.128 [c]
	6	40	14.000 ± 0.139 [c]
	24	40	14.100 ± 0.138 [c]
Sub-total (N-C)		120	14.067 ± 0.077
Total measurements		240	

h: hours; n: number; SE: Standard error; [abc]Means with different superscripts differ according to the test of minimal significant difference (MSD) (P<0.05)

TABLE V
Mitochondria Number. Descriptive statistics of each treatment

	Time (h)	n	Mean ± SE
Crotamine-like (C-L)	3	40	1.525 ± 0.080 [ab]
	6	40	1.275 ± 0.101 [b]
	24	40	0.325 ± 0.075 [c]
Sub-total (C-L)		120	1.042 ± 0.749
Normal control (N-C)	3	40	1.750 ± 0.117 [a]
	6	40	1.775 ± 0.121 [a]
	24	40	1.775 ± 0.127 [a]
Sub-total (N-C)		120	1.767 ± 0.070
Total measurements		240	

h: hours; n: number; SE: Standard error; [abc]Means with different superscripts differ according to the test of minimal significant difference (MSD) (P<0.05)

The number of mitochondrial cristae (FIG.10) under C-L effects showed a decrease at 6 and 24 h, which was statistically significant compared with the control. At 24 h an intense decrease in their number was noticed. This organelle is in charge of numerous chemical cellular reactions, such as cellular respiration, protein and electron transport and oxidative phosphorylation. Its cristae outline a membranous system that links with the internal mitochondria membrane in diverse segments facilitating the transport of metabolites and organic compounds to various parts of the organelle [28].

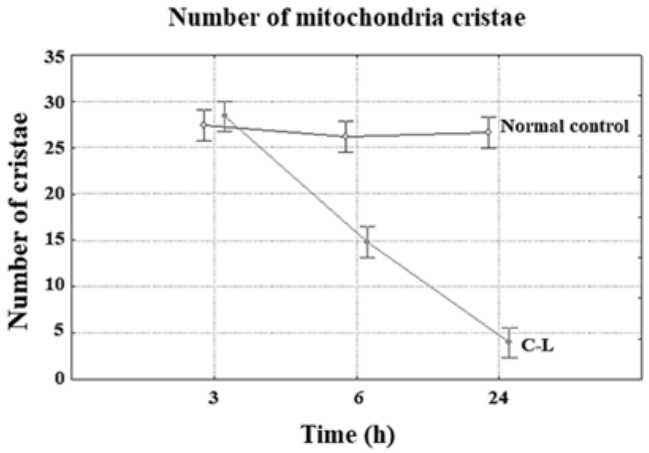

FIGURE 10. In the C-L effect on the number of mitochondria cristae was found significant differences in treatments (factor 1) P=0.00 and significant difference for the times (factor 2) P=0.00, with an interaction of P=0.00

TABLE VI
Areal Number Density of Mitochondria. Descriptive statistics of each treatment

	Time (h)	n	Mean ± SE
Crotamine-like (C-L)	3	40	0.151 ± 0.010 [c]
	6	40	0.346 ± 0.018 [b]
	24	40	0.439 ± 0.031 [a]
Sub-total (C-L)		120	0.312 ± 0.180
Normal control (N-C)	3	40	0.142 ± 0.009 [c]
	6	40	0.127 ± 0.008 [c]
	24	40	0.141 ± 0.009 [c]
Sub-total (N-C)		120	0.136 ± 0.005
Total measurements		240	

h: hours; n: number; SE: Standard error; [abc]Means with different superscripts differ according to the test of minimal significant difference (MSD) (P<0.05)

TABLE VII
Mitochondria Cristae. Descriptive statistics of each treatment

	Time (h)	n	Mean ± SE
Crotamine-like (C-L)	3	40	28.375 ± 0.751 [a]
	6	40	14.850 ± 0.944 [b]
	24	40	3.950 ± 0.443 [c]
Sub-total (C-L)		120	15.725 ± 11.059
Normal control (N-C)	3	40	27.459 ± 0.736 [a]
	6	40	26.211 ± 1.129 [a]
	24	40	26.617 ± 0.912 [a]
Sub-total (N-C)		120	26.762 ± 0.540
Total measurements		240	

h: hours; n: number; SE: Standard error; [abc]Means with different superscripts differ according to the test of minimal significant difference (MSD) (P<0.05)

TABLE VIII
Number Lipid Inclusions. Descriptive statistics of each treatment

	Time (h)	n	Mean ± SE
Crotamine-like (C-L)	3	40	0.428 ± 0.011 [a]
	6	40	0.320 ± 0.012 [b]
	24	40	0.167 ± 0.014 [c]
Sub-total (C-L)		120	0.305 ± 0.132
Normal control (N-C)	3	40	0.458 ± 0.008 [a]
	6	40	0.445 ± 0.008 [a]
	24	40	0.533 ± 0.089 [a]
Sub-total (N-C)		120	0.478 ± 0.030
Total measurements		240	

h: hours; n: number; SE: Standard error; [abc]Means with different superscripts differ according to the test of minimal significant difference (MSD) (P<0.05)

The number of lipid inclusions under C-L effects exhibited a decrease at 6 and 24 h (FIG. 11), which was statistically significant compared with the control. At 24 h an intense decrease in their number was observed. When observing the sequential changes on lipids, this decrease in the number of lipid inclusions of the studied cells could be explained by their utilisation, reflected by the increase in cortical activity under stress, which must begin during the first h post-injection of C-L.

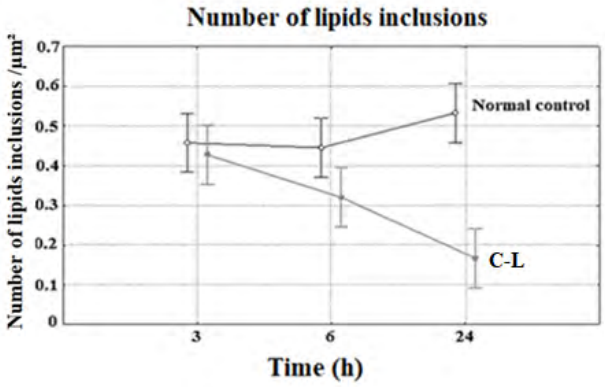

FIGURE 11. In the C-L effect on the number of lipid inclusions was found significant differences in treatments (factor 1) P=0.00 and significant difference for the times (factor 2) P=0.00, with an interaction of P=0.00

On the other hand, there was an increase in its areal number density of lipids inclusions after 6 h post C-L injection (FIG. 12), with high increase at 24 h. At first glance, the results obtained in both experiments could be contrasting, however, the decrease in the number of lipid inclusions and the increase in their areal number density are not necessarily correlative data [19]; these authors investigating Cushing syndrome, which is a hormonal disorder caused by prolonged exposure to an excess of cortisol (hormone produced by the adrenal glands)[15] explain that the increase in the area of lipid inclusions should be due to the increase in the activity of related enzymes in the uptake of low-density lipoprotein (LDL)-cholesterol, which could explain the data obtained regarding the alterations produced in lipid inclusions [34].

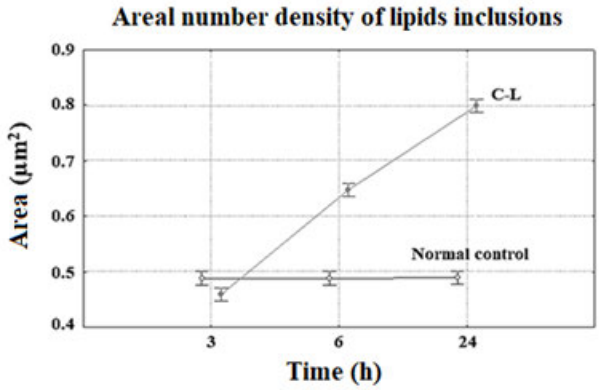

FIGURE 12. In the C-L effect on the real number density of lipids inclusions was found significant differences in treatments (factor 1) P=0.00 and significant difference for the times (factor 2) P=0.00, with an interaction of P=0.00

TABLE IX
Areal of Lipid Inclusions. Descriptive statistics of each treatment

	Time (h)	n	Mean ± SE
Crotamine-like (C-L)	3	40	0.460 ± 0.006 [d]
	6	40	0.647 ± 0.010 [b]
	24	40	0.800 ± 0.009 [a]
Sub-total (C-L)		120	0.636 ± 0.149
Normal control (N-C)	3	40	0.489 ± 0.001 [c]
	6	40	0.489 ± 0.001 [c]
	24	40	0.490 ± 0.001 [c]
Sub-total (N-C)		120	0.489 ± 0.001
Total measurements		240	

h: hours; n: number; SE: Standard error; [abcd]Means with different superscripts differ according to the test of minimal significant difference (MSD) (P<0.05)

Given the large presence of electrondense lipids in the results observed, it was possible to assume that there was a disorganisation in the activity of the smooth endoplasmic reticulum (SER), and based on this assumption it was focused on a more detailed study of SER.

SER covers approximately 80 % of some glandular cells, another reason for the importance of its observation during C-L action [36]. The diameter of the SER cisternae was dramatically increased from the early 3 h, reaching its maximum at 24 h (FIG. 13). This subcellular structure is responsible for the synthesis of molecules and the transport of substances. One of its functions is to deliver the proteins synthesised to the Golgi apparatus, which will transform and send them to the rest of the organisms. The C-L produced a strong reduction of the SER (data not shown), but the diameter of the cisternae was intensely increased at 6 and 24 h after C-L injection. Soulsby's work [32] indicated that the swelling of the SER cisternae was not necessarily related to increased activity. It should be remembered that the C-L could involve a final mitochondrial degeneration process, as seen previously in the mitochondrial alterations, this would compromise the production of energy (ATP), modifying the active transport of ions of the cell membrane and the sodium-potassium pump [17].

TABLE X
Diameter S.E.R. Descriptive statistics of each treatment

	Time (h)	n	Mean ± SE
Crotamine-like (C-L)	3	40	0.460 ± 0.006 [d]
	6	40	0.647 ± 0.010 [b]
	24	40	0.800 ± 0.009 [a]
Sub-total (C-L)		120	0.636 ± 0.149
Normal control (N-C)	3	40	0.489 ± 0.001 [c]
	6	40	0.489 ± 0.001 [c]
	24	40	0.490 ± 0.001 [c]
Sub-total (N-C)		120	0.489 ± 0.001
Total measurements		240	

h: hours; n: number; SE: Standard error; [abcd]Means with different superscripts differ according to the test of minimal significant difference (MSD) (P<0.05)

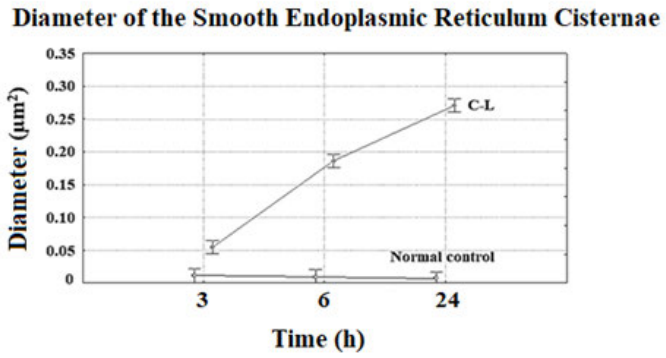

FIGURE 13. In the C-L effect on the diameter of the smooth endoplasmic reticulum (REL) cisternae was found significant differences in treatments (factor 1) P=0.00 and significant difference for the times (factor 2) P=0.00, with an interaction of P=0.00

The release of Ca^{2++} and the increase in its intra-mitochondrial concentration, further inhibit oxidative phosphorylation, consequently increasing anaerobic glycolysis and the accumulation of lactic acid in the cytoplasm, whereby the pH falls, thus multiplying the damage in the membranes and increased permeability.

PCA consisted of expressing a collection of variables in a set of linear combinations of factors not correlated with each other. This method allowed the original data (individuals and variables) to be represented in a space with a dimension less than the original space.

The analysis has great value for studies involving different variables [12] because it manages to create a multidimensional space where in this case it combines the 10 morphometric variables studied. This representation of 10 variables simultaneously analysed can be synthesised in a two-dimensional representation (FIG. 14) that comes from a true multidimensional graph; in the present case, the two-dimensional representation has significance because it has 95.85 % of the total variation of the multinational system (TABLE XI). In it, the differences of C-L to control were clearly observed, but unlike the other analyses that lead us to the same conclusion variable by variable, in this PCA analysis it is possible to observe the reality of 95.85 % of the phenomenon with the 10 variables studied and the effect of C-L in only 1 graph. The graphical representation of the PCA results and representation of different variables were shown in FIG. 14.

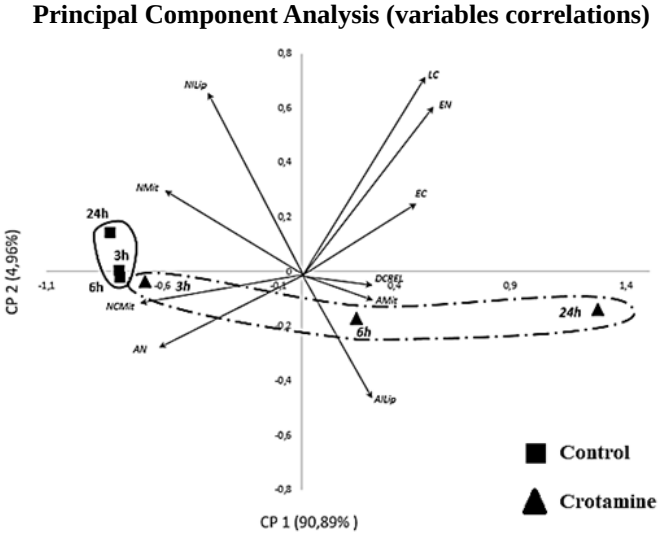

FIGURE 14. Graphical Representation of Principal Component Analysis (PCA). The points that describe the temporal performance (3, 6 and 24 h) of the control group (squares inside a continue line) and the crotamine-like protein (triangles inside line of points and dashes) are appreciated. The points of the coordinate system represent 95.85 % of the information synthesised in the 10 variables described: Areal number density of mitochondria (Mit-A); Number of the cristae (Mit-NC); Number of the mitochondria (Mit); Area of the nucleus (N-A); Number of Lipid Inclusions (Lip-NI); Areal number density of lipids inclusions (Lip-A); Diameter of cisternae of the smooth endoplasmic reticulum (SERcd); Thickening of the capillary endothelium (Ce); Capillary lumen (CL) and Nuclear envelope (Ne). The auto-vectors indicate the direction in which each variable (previously described) increases its magnitude.

The principal component 1 (PC1); X axis of FIG. 14 describes 90.89 % of the information (variable system) and the principal component 2 (PC2), Y axis; 4.9 % of this information (TABLE XI). The graph express 95.85 % of the variables, which is considered satisfactory.

TABLE XI
Principal Component

	PC 1	PC 2
Auto-values	9.089	0.496
Percentage	90.892	4.962
Accumulated percentage	90.892	95.854

The correlated variables are shown (TABLE XII). Thus. it is observed that there is a high positive correlation between the areal number density of mitochondria, the areal number density of lipids inclusions, the diameter of the cisternae of the smooth endoplasmic reticulum, the thickening of the capillary endothelium, the lumen of the capillary and the nuclear envelope on Axis 1; and positive correlation between the number of mitochondria, number of lipid inclusions, thickening of the capillary endothelium, capillary lumen and nuclear envelope on Axis 2

TABLE XII
Correlated Variables

PCA variables correlations	Axis 1	Axis 2
Areal number density of mitochondria (Mit-A)	0.325	-0.106
Cristae number (Mit-NC)	-0.328	-0.032
Mitochondria number (Mit)	-0.319	0.175
Nucleus Area (N-A)	-0.322	-0.208
Lipid Inclusions Number (Lip-NI)	-0.287	0.658
Areal number density of lipids inclusions (Lip-A)	0.322	-0.257
Diameter of the Smooth Endoplasmic Reticulum Cisternae (SERcd)	0.325	-0.075
Capillary Endothelium Thickening (Ce)	0.315	0.12
Capillary lumen (CL)	0.301	0.494
Nuclear Envelope (Ne)	0.316	0.388

CONCLUSIONS

In summary, this work point toward describing the quantitative and qualitative expressions of the general ultrastructural variations happening in the subcellular components of cells of envenomed mice, highlighting the crotamine-like action on the above mentioned cellular vital structures related to the cellular function, which play an essential protagonist role in the homeostasis and physiological regulation of the human body. In closing stages, even though muscle necrosis and/or apoptosis is the mainly substantial pathological problem associated with small myotoxins, such as crotamine, the search put forward that the medical impact of this molecule is related to their ability to cause intense damages at subcellular level, subject to their pharmacokinetic properties. In view of the above, it was concluded that the injection of C-L in mice induced acute inflammatory damages.

This toxin exhibited different sub-cellular targets, already talk over in the discussion as well as a number of activities, including neurotoxicity and myotoxicity. Its myotoxic capability feasibly is mainly related to the electrophysiological changes in sodium and potassium channels, changes in mitochondrial calcium homeostasis, alteration in the SER and degeneration of myofibrils, with resulting structural injury to muscle cells. Furthermore, investigations have revealed that the process of action of crotamine is not limited to the muscle tissue, if not, as it has seen in this work it involves other tissues, mainly adrenal gland, liver and kidneys. The cytotoxic effects of C-L have been demonstrated *in vivo* and *in vitro* employing adrenal gland cells and muscular motor endplate permitting the study of the mechanisms by which the C-L can modify cellular homeostasis by making injury to sub-cellular organelles such as mitochondria, SER, nucleus, and so on.

AUTHOR CONTRIBUTIONS

All experiments were performed at the Centro de Microscopia Electrónica, Facultad de Ciencias de la Universidad Central de Venezuela and the Laboratorio de Inmunoquímica y Ultraestructura, Instituto Anatómico de la Universidad Central de Venezuela, Caracas,

Venezuela. HJF, RG and ARA designed the study. EGL, RG and ARA performed the experiments. HJF, RG, EGL and ARA analysed and interpreted the data. EGL and ARA wrote the draft of the manuscript. All authors reviewed the manuscript and approved the final version for publication.

†During the evaluation process of this paper, Prof. Héctor. J. Finol passed away. Prof. Finol taught us his philosophical aspect of how to approach the study of cellular ultrastructure, in addition the devotion to his disciples and his general righteousness.

FINANCIAL SUPPORT (FUNDING)

The research was partially funding by grant from the Consejo de Desarrollo Científico y Humanístico de la Universidad Central de Venezuela (# PG: 09-8760-2013). Caracas. Venezuela.

ETHICAL STATEMENT

The project was accepted by the Institute of Anatomy Ethical Committee of the Universidad Central de Venezuela (April 26, 2019), under certification number: # 260420, carried out by the norms from the ARRIVE (EU Directive 2010/63/EU) for animal experiments guidelines, in agreement with the U.K. Animals (Scientific Procedures) Act, 1986 and associated guidelines.

DECLARATION OF COMPETING INTEREST

The people responsible for the completion of this paper declare that they have no competing financial interests to influence the work reported here. The funders had no responsibility in the plan of the study; in the assembly, scrutinises, or analysis of data; in the writing of the document, or in the resolution to publish the results

BIBLIOGRAPHIC REFERENCES

[1] AGUILAR, I.; GUERRERO, B.; SALAZAR, A.M.; GIRÓN, M.E.; PÉREZ, J.C.; SÁNCHEZ, E.E.; RODRÍGUEZ-ACOSTA, A. Individual venom variability in the South American rattlesnake *Crotalus durissus cumanensis*. **Toxicon.** 50: 214-224. 2007.

[2] REIS, L.P.G.; BOTELHO, A.F.M.; NOVAIS, C.R.; FIÚZA, A.T.L.; BARRETO, M.S.O.; FERREIRA, M.G.; BONILLA, C.; CHAVEZ-OLÓRTEGUI, C.; MELO, M.M. Cardiotoxic Effects of *Micrurus surinamensis* (Cuvier, 1817) Snake Venom. **Cardiovasc. Toxicol.** 21(6): 462-471. 2021.

[3] MACIEL, F.V.; RAMOS-PINTO, Ê.K.; VALÉRIO-SOUZA, N.M.; GONÇALVES DE A., T.A.; ORTOLANI, P.L.; FORTES-DIAS, C.L.; GARRIDO – CAVALCANTE, W.L. Varespladib (LY315920) prevents neuromuscular blockage and myotoxicity induced by crotoxin on mouse neuromuscular preparations. **Toxicon.** 30: 40-45. 2021.

[4] CHANG, C.; TSENG, K. Effect of crotamine, a toxin of South American rattlesnake venom on the sodium channel of murine skeletal muscle. **Br. J. Pharmacol**. 63: 551-559. 1978.

[5] OGUIURA, N.; BONI-MITAKE, M.; RÁDIS-BAPTISTA, G. New view on crotamine, a small basic polypeptide myotoxin from South American rattlesnake venom. **Toxicon.** 46(4): 363-370. 2005.

[6] FISHER, R.A. Statistical Methods for Research Workers. **Breakthroughs in Statistics.** In: Kotz, S.; Johnson, N.L. (Eds.). Springer Series in Statistics. Springer New York, NY. 601 pp. 1992.

[7] GINEBAUGH, S.P.; CYPHERS, E.D.; LANKA, V.; ORTIZ, G.; MILLER, E.W.; LAGHAEI, R.; MERINEY, S.D. The frog motor nerve terminal has very brief action potentials and three electrical regions predicted to differentially control transmitter release. **J. Neurosci**. 40: 3504-3516. 2020.

[8] GIRÓN, M.E.; PINTO, A.; FINOL, H.; AGUILAR, I.; RODRÍGUEZ-ACOSTA, A. Kidney structural and ultrastructural pathological changes induced by uracoan rattlesnake (*Crotalus vegrandis* Klauber 1941) venom. **J. Submicrosc. Cytol. Pathol**. 34: 447-459. 2002.

[9] GONÇALVES, J.M.; ARANTES, E.G. Estudos sobre venenos de serpentes brasileiras III—Determinação quantitativa de crotamina no veneno de cascavel Brasilera. **An. Acad. Bras. Cien**. 28: 369-371. 1956.

[10] HAYASHI, M.; NASCIMENTO, F.D.; KERKIS, A.; OLIVEIRA, V.; OLIVEIRA, E.B.; PEREIRA, A.; RADIS-BAPTISTA, G.; NADER, H.; YAMANE, T.; KERKIS, I.; TERSARIOL, I. Cytotoxic effects of crotamine are mediated through lysosomal membrane permeabilization. **Toxicon.** 52: 508-517. 2008.

[11] HERNÁNDEZ, M.; SCANNONE, H.; FINOL, H.J.; PINEDA, M.E.; FERNÁNDEZ, I.; GIRÓN, M.E.; AGUILAR, I; RODRÍGUEZ-ACOSTA, A. The crotoxin activity of rattlesnake venom (*Crotalus durissus cumanensis*) on the ultrastructure of cardiac atrial muscle**. Exp. Toxicol. Pathol.** 59: 129-137. 2007.

[12] JOLLIFFE, I.T.; CADIMA, J. Principal component analysis: a review and recent developments. **Philos. Trans. A. Math. Phys. Eng. Sci**. 374(2065): 2015-2020. 2016.

[13] KASTURIRATNE, A.; WICKREMASINGHE, R.; DE SILVA, N.; GUNAWARDENA, K.; PATHMESWARAN, A.; PREMARATNA, R.; SAVIOLI, L.; LALLOO, D.; DE SILVA, J. The global burden of snakebite: A literature analysis and modelling base on regional estimates of envenoming and deaths. **PLoS Med.** 5: e218. 2008.

[14] KERKIS, I.; HAYASHI, M.A.; PRIETO, D.A.; SILVA, A.R.; PEREIRA, A.; DE SÁ JR, P.L.; ZAHARENKO, A.J.; RÁDIS-BAPTISTA, G.; KERKIS, A.; YAMANE, T. State of the art in the studies on crotamine, a cell penetrating peptide from South American rattlesnake. **Biomed. Res. Int.** 2014: 675985. 2014.

[15] KLOSS, R.; GROSS, M.; FRANCIS, I.; DOROKIN, M.; SHAPIRO, B. Incidentally discovered adrenal mases. **Endocrine. Rev.** 16: 460-484. 1995.

[16] KONDRATSKYI, A.; KONDRATSKA, K.; SKRYMA, R.; PREVARSKAYA, N. Ion channels in the regulation of apoptosis. **Biochim. Biophys. Acta**. 1848: 2532-2546. 2015.

[17] LLOYD, R.; DOUGLAS, B.; YOUNG, W. Adrenal Gland. Endocrine disease. **Atlas of non-tumor pathology**: Editorial King D: AFIP, Washington DC (USA). Pp. 209-212. 2002.

[18] MONTGOMERY, D.C.; RUNGER, G.C. Probabilidades. **Probabilidad y Estadística Aplicadas a la Ingeniería**: McGraw-Hill, México, 895pp. 1996.

[19] NASCIMENTO, J.M.; FRANCHI, G.C. JR.; NOWILL, A.E.; COLLARES-BUZATO, C.B.; HYSLOP, S. Cytoskeletal rearrangement and cell death induced by *Bothrops alternatus* snake venom in cultured Madin-Darby canine kidney cells. **Biochem. Cell. Biol.** 85(5): 591-605. 2007.

[20] NICASTRO, G.; FRANZONI, L.; DE CHIARA, C.; MANCIN, A.; GIGLIO, J.; SPISNI, A. Solution structure of crotamine, a Na^+ channel affecting toxin from *Crotalus durissus terrificus* venom. **Eur. J. Biochem**. 270: 1969-1979. 2003.

[21] OGUIURA, N.; BONI-MITAKE, M.; RADIS-BAPTISTA, G. New view on crotamine, a small basic polypeptide myotoxin from South American rattlesnake venom. **Toxicon.** 46: 363-370. 2005.

[22] PEIGNEUR, S.; ORTS, D.J.B.; DA SILVA, A.R.P.; OGUIURA, N.; BONI-MITAKE, M.; DE OLIVEIRA, E.B.; ZAHARENKO, A.J.; DE FREITAS, J.C.; TYTGAT, J. Crotamine pharmacology revisited: Novel insights based on the inhibition of KV channels. **Mol. Pharmacol**. 82: 90–96. 2012.

[23] PONCE-SOTO, L.A.; MARTINS, D.; MARANGONI, S. Structural and Pharmacological Characterization of the Crotamine Isoforms III-4 (MYX4_CROCu) and III-7 (MYX7_CROCu) Isolated from the *Crotalus durissus cumanensis* Venom. **Toxicon**. 55: 1443-1452. 2010.

[24] PONCE-SOTO, L.A.; MARTINS-DE-SOUZA, D.; NOVELLO, J.C.; MARANGONI, S. Structural and biological characterization of two crotamine isoforms IV-2 and IV-3 isolated from the *Crotalus durissus cumanensis* venom. **Protein J.** 26: 533-540. 2007.

[25] PULIDO, M.; RODRIGUEZ-ACOSTA, A.; FINOL, H.J.; AGUILAR, I.; GIRÓN, M.E. Ultrastructural pathology in skeletal muscle of mice envenomed with *Crotalus vegrandis* venom. **J. Submicrosc. Cytol. Pathol**. 31: 555-561. 1999.

[26] RADIS-BAPTISTA, G.; OGUIURA, N.; HAYASHI, M.A.F.; CAMARGO, M.E,; GREGO, K.F.; OLIVEIRA, E.B.; YAMANE, T. Nucleotide sequence of crotamine isoform precursors from a single South American rattlesnake (*Crotalus durissus terrificus*). **Toxicon.** 37: 973-984. 1999.

[27] RENGIFO, C.; RODRÍGUEZ-ACOSTA, A**.** Capitulo III**. Serpientes veneno y tratamiento médico en Venezuela:** Fondo Editorial de la Facultad de Medicina, Universidad Central de Venezuela Caracas, Venezuela. 272 pp. 2019.

[28] REYES-JUÁREZ, J.L.; ZARAIN-HERZBERG, Á. Función del retículo sarcoplásmico y su papel en las enfermedades cardíacas. **Arch. Cardiol. Mex**. 76: 18-32. 2006.

[29] SÁNCHEZ, E.E.; GONZÁLEZ, R.; LUCENA, S.; GARCÍA, S.; FINOL, H.J.; SUNTRAVAT, M.; GIRÓN, M.E.; FERNÁNDEZ, I.; RODRÍGUEZ-ACOSTA, A. Crotamine-like from Southern Pacific rattlesnake (*Crotalus oreganus helleri*) Venom acts on human leukemia (K-562) cell lines and produces ultrastructural changes on mice adrenal gland. **Ultrastruc. Pathol**. 42: 116–123. 2018.

[30] SIEBER, M.; BOSCH, B.; HANKE, W.; FERNANDES-DE LIMA, V.M. Membrane-modifying properties of crotamine, a small peptide-toxin from *Crotalus durissus terrificus* venom. **Biochim. Biophys. Acta**. 1840: 945-950. 2014.

[31] SOKAL, R.R.; ROHLF, F.J. Biometry. **The Principles and Practice of Statistics in Biological Research**: Freeman WH and Company San Francisco (USA), 253 pp. 2012.

[32] SOULSBY, E.J. The Sir Frederick Hobday Memorial Lecture. We don't shoot horses anymore. **Equine Vet. J.** 20 (Supl. 4): 243-248. 1981.

[33] STOSCHECK, C.M. Quantitation of protein. **Methods. Enzymol.** 182:50–68. 1990.

[34] TISHENINA, R.S.; KALININ, A.P.; KOZLOVA, N.K. Bolezn' Itsenko-Kushinga i perekisnoe okislenie lipidov [Itsenko-Cushing disease and lipid peroxidation]. **Probl. Endokrinol. (Mosk).** 34: 32–36. 1988.

[35] TOYAMA, M.H.; CARNEIRO, E.M.; MARANGONI, S.; BARBOSA, R.L.; CORSO, G.; BOSCHERO, A.C. Biochemical characterization of two crotamine isoforms isolated by a single step RP-HPLC from *Crotalus durissus terrificus* (South American rattlesnake) venom and their action on insulin secretion by pancreatic islets. **Biochim. Biophys. Acta.** 1474: 56-60. 2000.

[36] WANG, X.; KOMATSU, S. Isolation, purity assessment, and proteomic analysis of Endoplasmic Reticulum. **Methods. Mol. Biol**. 2139: 117-131. 2020.

[37] WANG, Y.; HEKIMI, S. Mitochondrial dysfunction and longevity in animals: Untangling the knot. **Sci**. 350: 1204-1207. 2015.

[38] BRUNI, V.; CARDINALI, M.L. VITULANO', D. A Short Review on Minimum Description Length: An Application to Dimension Reduction in PCA. **Entropy (Basel).** 24(2): 269-285. 2022.